Physicochemical aspects of lead bioaccumulation by Chlorella vulgaris

Slaveykova, Vera; Wilkinson, Kevin J

Environ. Sci. Technol. **2002**, *36,* 969−975

Physicochemical Aspects of Lead Bioaccumulation by *Chlorella vulgaris*

VERA I. SLAVEYKOVA* AND KEVIN J. WILKINSON

Analytical and Biophysical Environmental Chemistry (CABE), University of Geneva, Sciences II, 30 Quai Ernest Ansermet, 1211 Geneva 4, Switzerland

The relationship between lead speciation and its bioaccumulation by the alga *Chlorella vulgaris* was studied in the absence and presence of nitrilotriacetic, iminodiacetic, malonic, and citric acids. Pb uptake fluxes were rigorously analyzed by considering the simultaneous effects of metal transport in the medium coupled with metal complex dissociation kinetics. Under the conditions examined here, lead biouptake by *C. vulgaris* was governed by the free lead ion activity. Potentially labile hydrophilic complexes such as lead citrate and lead malonate did not contribute to the internalization fluxes. Kinetic modeling of the mass transport, adsorption reactions, and internalization fluxes confirmed the rate limiting role of the internalization flux. Comparison of the internalization and diffusive fluxes revealed that even in the presence of a large excess of Pb complexes, the supply of free ion (Pb^{2+}) was sufficient to account for the observed Pb uptake. Pb adsorption to the cell surface was described by Langmuir isotherm. A new method was proposed as a means to estimate the number of Pb occupied transport sites at steady state. The apparent stability constant for the interaction of Pb with transport sites was determined to be $10^{5.5}$ M^{-1} at pH 6. Low temperature decreased both the Pb uptake flux and the Pb adsorbed to the transport sites. Pb uptake in the presence of Ca was competitively inhibited, and the binding affinity constant for Ca and transport sites was estimated to be $10^{4.67}$ M^{-1} at pH 6. Results were discussed within the perspective of the free ion activity and biotic ligand models.

Introduction

The interaction of trace elements with aquatic organisms generally involves several consecutive processes including (*1*−*4*) the following: (i) mass transfer to the biological interface, (ii) diffusion through the solution boundary layer and protective layers around the organism (e.g., mucus, cell wall), (iii) adsorption at the biological surface (both to transport sites and biologically inert sites), and (iv) transport across the biological membrane (Figure 1). Any of these steps has the potential to be the rate-limiting process (i, refs *5* and *6*; ii, refs *7* and *8*; iii, refs *3* and *4*; iv, refs *9* and *10*) depending on the microorganism, the nature and speciation of the accumulated element, and the physicochemistry of the medium including pH, water hardness, etc. A complete description of the above processes is extremely complicated and dependent on a large number of assumptions, not all of which are reasonably satisfied in real systems.

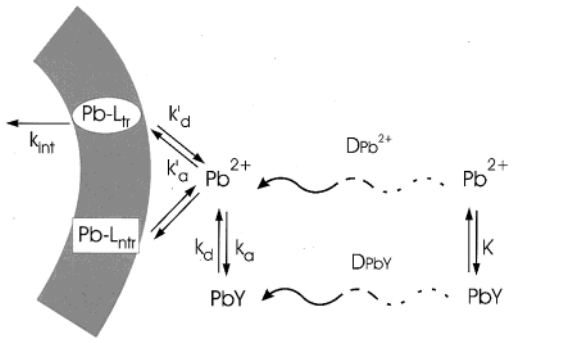

FIGURE 1. Schematic representation of the lead uptake process. Simplified flux equations for physical and biological transport and chemical reactions are given in Table 2.

For the most part, much of the recent literature examining relationships between chemical speciation and biological availability has assumed the applicability of the free-ion activity model (FIAM) or more recently the biotic ligand model (BLM). The underlying assumption of both models is that equilibrium among the metal species in solution and those bound to sensitive sites (e.g., receptors) on the membrane (*10*, *11*) is attained. This implies that the first step of the uptake process is a rapid and reversible adsorption to the biological surface that is most often followed by first-order, rate-limiting internalization. The two-phase process at steady state can also be described by a Michaelis−Menten hyperbolic equation (*12*).

In most investigations, biological effects are often simply correlated with trace metal speciation. Because effects are rarely linearly related to uptake fluxes and since free ion concentrations are often co-varied with other chemical species, this experimental design does not allow for verification of the underlying model. Although more general conceptual trace metal uptake models also exist (e.g., refs *1*−*4*, *13*, and *14*), many of their assumptions have not been rigorously examined. Recently, van Leeuwen (*13*) has proposed a more general approach in which the relationship between trace metal speciation and bioavailability has been analyzed on the basis of the dynamics of mass transport and the association/dissociation reactions in complexing external media. The resulting steady-state fluxes have been expressed in terms of relative bioaffinity parameters and ratios between maximal uptake fluxes and transport fluxes. Among the other results, it was shown (*15*) that biouptake fluxes could be influenced by the size of the microorganisms, due both to an increase in the diffusive flux and to a decrease in complex lability in the transition from linear to radial diffusion for small organisms. Lead uptake was examined theoretically as an example of a metal with relatively fast association−dissociation kinetics (*15*, *16*) so that a steady state between the metal species in the solution and the metal bound to the transport sites might be expected (*2*). The detailed theoretical analysis revealed that, under certain conditions, the diffusive transport flux could be rate limiting or that labile complexes could contribute to the biouptake flux. Unfortunately, only limited experimental evidence is currently available to verify the above theoretical predictions.

Therefore, the objective of this paper was to study as rigorously as possible the relationship between lead speciation and the corresponding biouptake fluxes. The study

* Corresponding author phone: +41 22 702 6445; fax: +41 22 702 6069; e-mail: vera.slaveykova@cabe.unige.ch.

10.1021/es0101577 CCC: $22.00
Published on Web 01/31/2002

was designed to test the assumptions of the existing simplified models in order to provide quantitative data that can be used to evaluate the models and to indicate future directions for experiments designed to better understand the uptake process. The influence of Pb complex lability, temperature, and Ca on the adsorption to transport sites and subsequent Pb uptake was also examined. A critical parameter for the transport models, i.e., Pb bound to transport sites, was determined experimentally and distinguished from Pb not related to the internalization process.

Materials and Methods

Pb accumulation by *Chlorella vulgaris* was examined in the absence and presence of hydrophilic complexes of increasing lability (decreasing stability): nitrilotriacetic (NTA), iminodiacetic (IDA), citric, and malonic acids for Pb^{2+} concentrations in the range of 5×10^{-9}–5×10^{-5} M.

The spherical unicellular green algae *C. vulgaris* (strain UTCC 266) was employed in this study mainly due to the relative ease by which it is possible to culture and control its metabolic state, size, and surface area distribution. *Chlorella* was cultured in OECD medium (*17*) in an incubation chamber (Infors) at 22 °C, under a 12:12 h light:dark regime, 50 μmol of photons m^{-2} s^{-1} fluorescent lighting, and rotary shaking (100 rpm). Cells in their mid-exponential phase were harvested by gentle filtration, washed, and resuspended in a solution of 10^{-2} M MES (2-(*N*-morpholino)ethanesulfonic acid, Sigma) at pH 6, containing known quantities of Pb and ligands. Under these conditions, in the absence of added ligand, the free lead ion (Pb^{2+}) represented >97% of total Pb in solution.

Surface-bound Pb was distinguished from cellular Pb using a 1-min extraction in 10^{-2} M EDTA (ethylenediaminetetraacetic acid, Fluka) (*18*). Cellular Pb was determined after digestion of the filtered, EDTA-washed algae with 1 mL of concentrated, ultrapure HNO_3 (Baker). Dissolved Pb was determined from filtrate sampled prior to the EDTA wash, and adsorbed Pb was quantified from the EDTA wash solution. NTA and CDTA (*trans*-1,2-diaminocyclohexane-*N*,*N*,*N*′,*N*′-tetraacetic acid, Fluka) were also tested as washing agents. All three Pb fractions (dissolved, adsorbed, cellular) were measured by atomic absorption spectrometry (flame or electrothermal) or by inductively coupled plasma mass spectrometry depending on the concentrations. Experimentally obtained plots of cellular Pb as a function of accumulation time were used to obtain internalization fluxes. Uptake was examined in short-term experiments (maximum 60 min) to reduce the effect of efflux, exudate production, or variable cell sizes and numbers. For each experimental point, cell densities, sizes, and surface distributions were determined using a Coulter Multisizer II particle counter (50 μm orifice, Coulter Electronics). Experiments were performed with algae with a mean cellular diameter of 3.6 μm and a cell density between 8×10^6 and 1×10^7cell mL^{-1}.

Lead speciation in the medium was determined by theoretical calculations using MINEQL$^+$ (version 3.01a) using updated constants (*19*–*21*) and a correction for the ionic strength of the solutions using the Davies equation. Kinetic modeling experiments were performed using Berkley Madonna modeling software (version 7.0). Initial parameters for the model were determined experimentally using steady-state equations taken from the literature (*1*, *13*).

Results and Discussion

Pb Adsorption by *Chlorella vulgaris*. Short-term uptake experiments typically showed a rapid, steady-state adsorption (EDTA-extractable Pb) and a slow, linear internalization (non-EDTA-extractable Pb) (e.g., Figure 2). The nonzero intercept of cellular Pb will be discussed later in the text. The observation of a rapid plateau value of adsorbed Pb supported

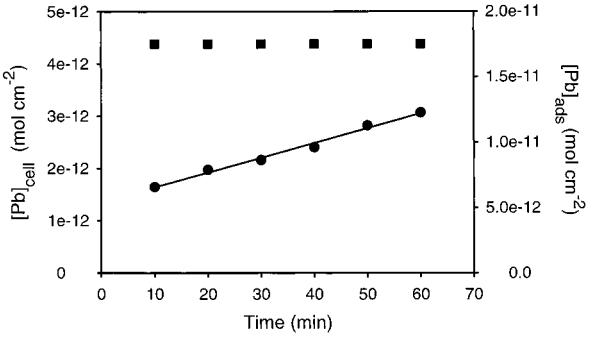

FIGURE 2. Adsorbed (■, EDTA extractable) and cellular lead (●, non-EDTA extractable) as function of accumulation time. Pb in the presence of NTA, pH 6; $[Pb]_{tot} = 10^{-5}$ M; $[Pb^{2+}] = 2.5 \times 10^{-7}$ M.

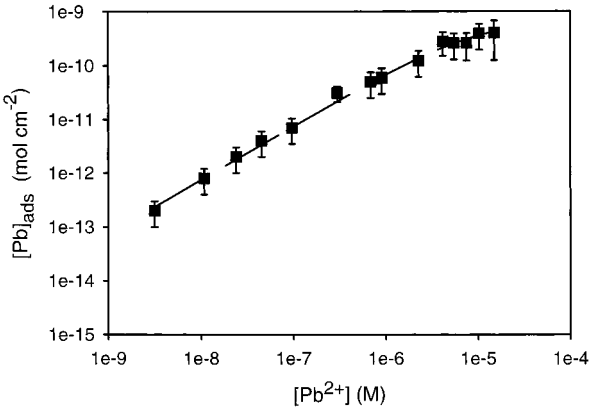

FIGURE 3. Logarithmic representation of adsorbed (■, EDTA extractable) lead as a function of $[Pb^{2+}]$. A Langmuir isotherm is presented as a dashed line for K_{ads} $10^{5.04}$ M^{-1} and $\{L_{tot}\} = 6.6 \times 10^{-10}$ mol cm^{-2}.

the assumption that equilibrium was attained between the external solution and the cell surface. Other experiments in our laboratory have shown that adsorption occurred faster than it was possible to accurately measure using this protocol (i.e., minimum filtration time of ca. 1 min). The amount of adsorbed Pb increased with the concentration of Pb^{2+}, attaining saturation at values larger than about 1×10^{-5} M (Figure 3). Using a Langmuir adsorption isotherm, the concentration of total Pb binding sites, $\{L_{tot}\}$, was determined to be $(6.6 \pm 1) \times 10^{-10}$ mol cm^{-2} with a conditional adsorption constant of $10^{5.04}$ M^{-1} (pH 6). The conditional adsorption constant and total site concentration determined in this manner takes into account both membrane transport proteins, L_{tr}, and sites that did not participate in the internalization process, including cell wall polysaccharides, peptidoglycans, etc.

Pb Internalization Fluxes by *Chlorella vulgaris*. Internalization fluxes (J_{int}) were determined for 5×10^{-9}–5×10^{-5} M Pb^{2+} in the absence and presence of NTA, IDA, citric, and malonic acids. Each data point in Figure 4 corresponds to the slope obtained from an uptake experiment of cellular Pb versus time (similar to the circles in Figure 2) and is the mean of a minimum of three replicate experiments. The addition of ligands to the experimental solutions lead to a significant decrease of cellular Pb that was correlated to the free lead ion and not to the total lead concentration. Although some low molecular weight ligands such as citric acid have been shown to enhance the metal uptake and toxicity (*9*, *22*), given the observed results and the short accumulation times, there is no reason to believe that this is occurring here.

The observed linear increase of cellular Pb with time (Figure 2) corresponded well to results that would be predicted by the FIAM (*9*, *10*, *12*). In addition, the FIAM

TABLE 1. Lability Criterion (L[a]) Estimated in the Presence of Several Ligands at pH 6[b]

ligand Y	NTA[c]		malonic acid		citric acid		IDA	
$[Y]_{tot}$, M	5×10^{-6}	5×10^{-5}	5×10^{-3}	1×10^{-2}	1×10^{-3}	5×10^{-3}	1×10^{-3}	1×10^{-2}
μ, cm	6×10^{-5}	1.5×10^{-5}	8×10^{-8}	1×10^{-7}	7×10^{-8}	8×10^{-8}	4×10^{-6}	9×10^{-6}
L	8×10^{-2}	3×10^{-2}	5×10^{2}	3×10^{2}	4×10^{2}	2×10^{2}	11	1

[a] Formation of a 1:1 complex was considered. Values of $L \gg 1$ indicate that complexes are labile and therefore may, under certain circumstances, contribute to the uptake flux. Values of $L \ll 1$ indicate behavior corresponding to nonlabile complexes. [b] Lability criterion $L = \mu r k_d / D_{PbY}$ as operationally defined for condition of radial diffusion and linear association−dissociation kinetics (*16*). $\mu = (D_{PbY}/(k_a c_Y))^{1/2}$ reaction layer thickness; D_{PbY} = diffusion coefficient of PbY complex; c_Y = ligand concentration; r = radius of the microorganism; k_a = formation rate constant; k_d = dissociation rate constant, $k_d = k_a/K$; K = stability constant of PbY complex. [c] $[Pb]_{tot}$ 5×10^{-7} M.

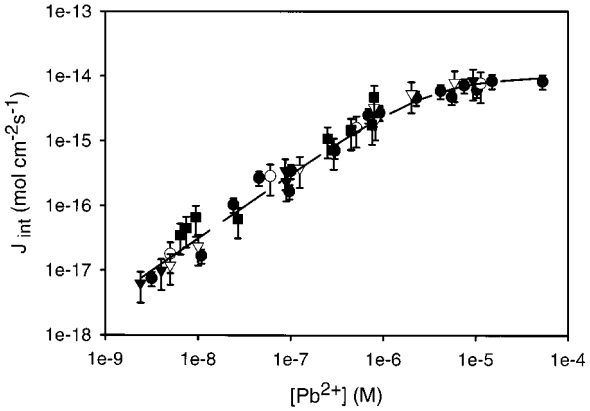

FIGURE 4. Logarithmic representation of internalization fluxes as a function of $[Pb^{2+}]$ in the absence (●) or presence of ligand: (■) NTA, (▼) citric acid, (○) IDA, and (▽) malonic acid. Dashed line represents a Michaelis−Menten plot for $K_M = 3 \times 10^{-6}$ M and $J_{max} = 1 \times 10^{-14}$ mol cm^{-2} s^{-1}. Standard deviations are given when larger than the symbol size.

predicts that the uptake fluxes should be linearly related to bulk free metal ion concentration, $[M^{z+}]$, i.e., J_{int} = constant × $[M^{z+}]$; or in other words, that membrane permeability ($P = J_{int}/[M^{z+}]$) is constant. On a log J_{int}−log$[M^{z+}]$ graph, a slope of 1 must be observed to validate the FIAM. Indeed, in Figure 4, a linear increase of J_{int} with $[Pb^{2+}]$ (slope of 1 on the log−log graph) and a well-pronounced saturation plateau at higher concentrations was observed. The uptake results were fitted with the Michaelis−Menten equation (dashed line on Figure 4). The apparent half-saturation constant (K_M) and the maximal internalization flux (J_{max}) were determined to be $(3.0 \pm 0.5) \times 10^{-6}$ M and $(1.0 \pm 0.2) \times 10^{-14}$ mol cm^{-2} s^{-1}, respectively. Using an experimentally determined cell radius of 1.8×10^{-4} cm, this corresponds to a maximal internalization flux of approximately 4×10^{-21} mol of Pb cell^{-1} s^{-1}. Maximum internalization fluxes obtained for $[Pb^{2+}]$ larger than about 1×10^{-5} M were equal in the absence or presence of ligand. The existence of a single saturation plateau supports the hypothesis that internalization was predominantly via a single transporter. Membrane permeability to Pb, calculated from the linear dependence between J_{int} and $[Pb^{2+}]$ at $[Pb^{2+}] < K_M$ was estimated to be $(3.3 \pm 0.5) \times 10^{-6}$ cm s^{-1}.

Determination of Pb Complex Lability. By definition, inert complexes do not contribute to the metal supply towards a biological surface. Complexes are defined as labile when they can form and dissociate many times during their transport through the diffusion layer, with the resulting metal supply to the biological surface potentially determined by both free metal and labile species (*13*, *23*). For a given complex, the lability criteria (Table 1) represents the ratio of the flux that would result from a kinetically limited dissociation of the complex to the rate of metal supply by a purely diffusion controlled flux (see also Figure 1) (*13*, *15*, *16*). The validity of this equation, the basic assumptions for its derivation, and its applicability to microorganisms have been discussed previously (*13*, *15*). In our case, calculations were performed with an experimentally determined mean radius for *C. vulgaris* of 1.8 μm and under conditions where the 1:1 complex predominated.

Theoretical estimations of the lability criterion (L) revealed that labile behavior ($L \gg 1$) was expected in the presence of citric and malonic acid while NTA complexes were nonlabile ($L \ll 1$) and therefore not expected to contribute to the uptake fluxes (Table 1). Pb−IDA complexes are predicted to be a borderline case ($L \approx 1$). Nonetheless, the expected behavior of the labile complexes with respect to the biouptake fluxes is not straightforward since it also depends on the "demand" of the organism (*13*, *15*). If the free metal supply to the organism is sufficient to sustain uptake, then no contribution of the labile complexes is predicted.

Influence of Complex Lability on Pb Internalization Fluxes. In the presence of labile Pb complexes (citric and malonic acids, Table 1), uptake fluxes were proportional to $[Pb^{2+}]$ rather than total lead concentrations, indicating that the labile metal complexes did not contribute to the uptake fluxes. Indeed, determinations indicating that the maximal internalization flux (J_{max}) was much smaller than maximal theoretical diffusive flux, J_{dif} ($J_{dif} = 5.2 \times 10^{-14}$ mol cm^{-2}s^{-1} for 1×10^{-9} M Pb, equations from Table 2) demonstrated that no mass transfer limitation could be expected for any of the conditions that were examined (*13*, *15*). In this case, the activity/concentration of Pb^{2+} should govern the interaction with the surface transport ligand sites and consequently the bioavailability of Pb in the medium. Using a similar logic, it was possible to estimate that mass transfer could be limiting (bioconversion parameter = $J_{max}/J_{dif} > 10$) for total [Pb] < 1.9×10^{-11} M, concentrations that are generally smaller than those observed in natural waters (*23*).

In the presence of ligands forming labile complexes, such as citric and malonic acid, the ratio of the maximal internalization flux to the diffusive flux must also be considered with respect to the degree of complexation (*13*, *15*). The calculations indicated that not only was $J_{max} < J_{dif}$ but also J_{max}/J_{dif} was smaller than $[Pb^{2+}]/[Pb]_{tot}$. In this case, the maximal internalization flux was already much smaller than the limiting supply of free ions, suggesting that the turnover rate of transport proteins was so slow that the available $[Pb^{2+}]$ was sufficient to satisfy algal demand (in a chemical sense). This observation is not completely unexpected given the lack of known biological demand for Pb. Although labile species did not contribute to Pb internalization fluxes under the conditions examined here, it was possible to predict that, for $[Pb^{2+}]/[Pb]_{tot} = 0.1$, labile species could contribute to the uptake fluxes at total Pb concentrations of 1.9×10^{-9} M.

Characterization of the Transport Sites. A special feature of the lead uptake process is that a significant y-intercept was consistently observed in the plots of cellular lead versus time (e.g., Figure 2). These values were reproducible and significantly larger than algal control digests (algae prior to Pb addition) and blank values of the acid and filter. Although it might be possible to explain the intercept by a rapid initial

TABLE 2. Biological and Physicochemical Fluxes Used To Predict Pb Accumulation by *Chlorella vulgaris* (see also Figure 1)

flux	mathematical expression	parameter	initial value or range
diffusive flux	$J_{dif} = D_{Pb^{2+}}([Pb]_b - [Pb]_i)(1/\delta + 1/r)$	$D_{Pb^{2+}}$, diffusion coefficient of Pb^{2+} ($cm^2\ s^{-1}$)	9.5×10^{-6}
		δ, diffusion layer thickness (cm)	20×10^{-4}
		r, radius of the microorganism (cm)	1.8×10^{-4}
		$[Pb]_b$, bulk Pb^{2+} concn (M)	variable
		$[Pb]_i$, Pb^{2+} concn at interface (M)	
adsorption−desorption flux to transport sites	$J_{ads,tr} = k_a[Pb^{2+}][L_{tr}]$	k_a, formation rate constant ($M^{-1}\ s^{-1}$)	$>10^2$−10^4 and $<10^{13}$ (Eigen mechanism)
		k_d', dissociation rate constant (s^{-1})	$>10^{-3}$−10^{-2}
	$J_{des,tr} = k_d'[Pb{-}L_{tr}]$	K_{Pb-tr}, stability constant of $Pb{-}L_{tr}$ (M^{-1})	$>3.3 \times 10^5$
		$[L_{tr}]$, free transport site surface concn (mol cm^{-2})	
		$[L_{tr}] = [L_{tr,tot}] - [Pb{-}L_{tr}]$	
		$[Pb{-}L_{tr}]$, transport site bound Pb concn (mol cm^{-2})	
		$[L_{tr,tot}]$, total transport site surface concn (mol cm^{-2})	5×10^{-12}−5×10^{-11}
internalization flux	$J_{int} = k_{int}[Pb{-}L_{tr}]$	k_{int}, internalization constant (s^{-1})	2×10^{-4}−2×10^{-3}

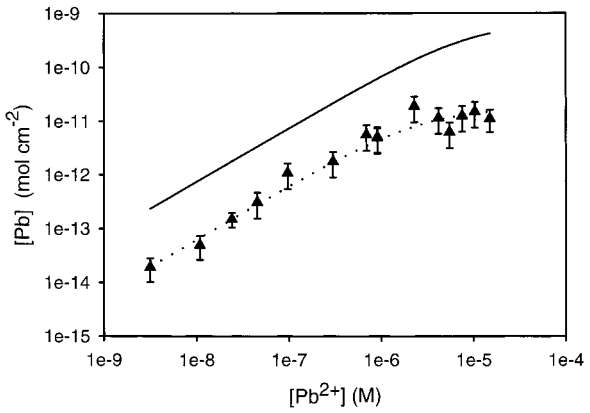

FIGURE 5. Logarithmic representation of Pb bound to transport sites (▲, obtained as the intercept from a Pb_{cell} vs time plot) as function of $[Pb^{2+}]$. The Langmuir isotherm is presented as a dotted line for K_{ads} $10^{5.54}$ M^{-1} and $\{L_{tr,tot}\} = 1.5 \times 10^{-11}$ mol cm^{-2}. For comparative purposes, the Langmuir isotherm describing total adsorbed Pb from Figure 3 is presented as a solid line. Standard deviations are given when larger than the symbol size.

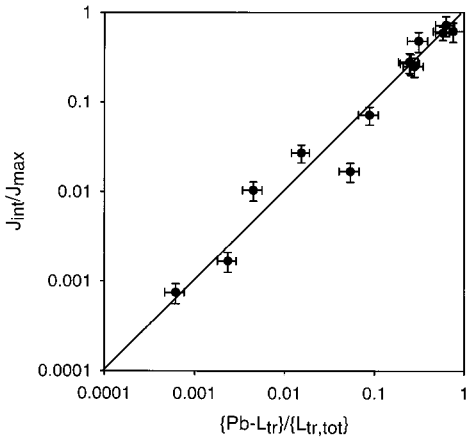

FIGURE 6. Logarithmic representation of normalized uptake fluxes, J_{int}/J_{max}, as a function of the ratio of occupied to total transport sites, $\{Pb{-}L_{tr}\}/\{L_{tr,tot}\}$, in the absence of complexing agent (slope = 1.01, $R^2 = 0.93$). Standard deviations are given when larger than the symbol size.

accumulation of Pb by the cell, experiments for which accumulation data was obtained at 1 min had a near identical intercept. It was hypothesized that the experimentally determined intercepts corresponded to the rapid formation of a Pb surface complex and therefore could be used as a surrogate for the concentration of Pb-bound receptor sites, $\{Pb{-}L_{tr}\}$.

Several further observations lent support to the above hypothesis. First, the intercepts increased linearly with $[Pb^{2+}]$. In addition, values tended to saturation at higher concentrations (Figure 5) such that intercepts determined at the maximal uptake flux values were constant. Using a Langmuir isotherm, the total number of intercept determined sites, $\{L_{tr,tot}\}$, was calculated to be about $(1.5 \pm 0.5) \times 10^{-11}$ mol cm^{-2}, a value about 60 times smaller than the estimate of total adsorption sites $\{L_{tot}\}$ determined earlier. This value of $\{L_{tr,tot}\}$ corresponded to about 3.7×10^6 transport sites potentially available for Pb for each cell. Typical receptor concentrations range from 10^4 to 10^6 $cell^{-1}$ (*24*). Calculations of the surface area required to adsorb 1.5×10^{-11} mol cm^{-2} of Pb on the cell transport sites at saturation indicated that about 0.3% of the algal surface would be covered by Pb (assuming that adsorbed Pb has the same dimension as the hydrated ion).

In addition, the apparent stability constant determined by the Langmuir treatment using intercept values as a surrogate for the binding of Pb to the transport sites was calculated to be $10^{5.54}$ M^{-1} (Figure 5). This estimate of K_{Pb-tr} is almost identical to the reciprocal value of the Michaelis−Menten constant, $10^{5.52}$ M^{-1}, lending convincing support to the hypothesis that the intercept could be used as a measure for occupied transport sites since $K_M = (k_d + k_{int})/k_a$ so that for $k_{int} \ll k_d$, $K_M \approx 1/K_{tr}$. Finally, the fraction of apparent occupied transport sites (ratio between occupied $\{Pb{-}L_{tr}\}$ and total $\{L_{tr,tot}\}$ transport sites) (*24*) was well correlated (slope = 1.01 and $R^2 = 0.93$) to the normalized uptake flux J_{int}/J_{max} over 3 orders of magnitude (Figure 6).

Knowledge of the transport site concentration allows the determination of the internalization rate constant (k_{int}) for the transfer of bound metal across the membrane. At low $[Pb^{2+}]$, lead uptake fluxes are directly proportional to Pb^{2+} activities in solution due to a proportionality with the concentration of the surface complex ($J_{int} = k_{int}\{Pb{-}L_{tr}\}$). Values of k_{int} can also be obtained by using saturation values of the Michaelis−Menten plot ($J_{max} = k_{int}\{L_{tr,tot}\}$). The value of k_{int} was similar in both cases, estimated to be about 4.3 $\times 10^{-4}$ s^{-1} for the linear and 6.6×10^{-4} s^{-1} for the saturation regime.

Influence of Extraction Parameters on Cellular Pb. It is clear that values of the intercept (and in turn cellular Pb) were in part operationally defined by the EDTA contact times employed in the extraction procedure. To gain additional insight into the desorption process, the role of contact times and complex stability were examined for EDTA, NTA, and CDTA washes. Cellular and desorbed Pb was determined for algae preexposed for 15 min to 2.2×10^{-6} M Pb. The concentration of cellular (post-washed) Pb was independent

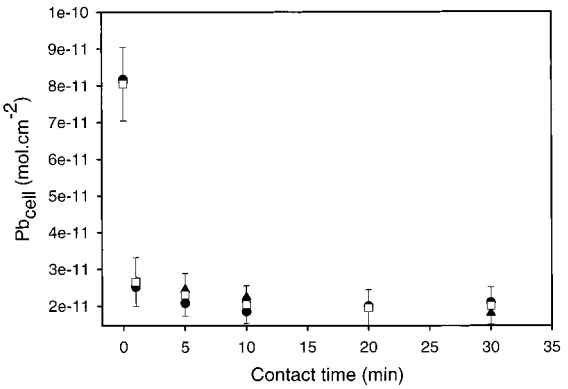

FIGURE 7. Cellular Pb as a function of contact time with the wash solution: 10^{-2}M EDTA (●), 10^{-2} M NTA (▲), and 10^{-2} M CDTA (□). Accumulation time was 15 min in [Pb] = 2.2×10^{-6} M.

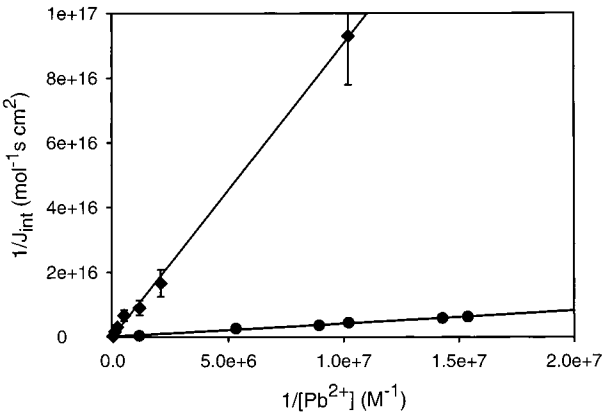

FIGURE 8. Lineweaver−Burk linear transformation plots for Pb internalization in the absence (●) or presence (◆) of 5×10^{-4} M Ca. Standard deviations are given when larger than the symbol size.

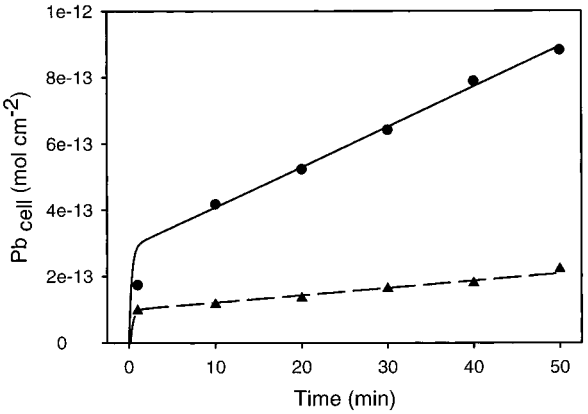

FIGURE 9. Cellular Pb as a function of time at 22 (●) and 2 °C (▲) for [Pb^{2+}] = 9.7×10^{-8} M. The solid line given for the data at 22 °C corresponds to the numerical simulation results for optimized parameters of $k_{int} = 7 \times 10^{-4}$ $s^{-1}$and $K_{tr} = 3 \times 10^5$ M^{-1} while the dashed line corresponds to data at 2 °C ($k_{int} = 3.6 \times 10^{-4}$ s^{-1} and $K_{tr} = 7 \times 10^4$ M^{-1}).

of the ligand used for the extraction, despite a variation in their conditional stability constants (pH 6) of 10^8 ($K'_{Pb-NTA} = 10^{7.3}$, $K'_{Pb-EDTA} = 10^{13}$; $K'_{Pb-CDTA} = 10^{15.3}$; *19*). Furthermore, the relatively small values of K_{Pb-tr}, especially when compared to the large stability constants of these complexes, lends support to the hypothesis that slow decomplexation kinetics rather than thermodynamic arguments are responsible for observed positive intercept.

A slight decrease in cellular Pb was observed as a function of contact times between 1 and 30 min for all extractions (Figure 7). Further increases in the contact times to 120 min did not produce significant changes in the cellular Pb. Although internalization fluxes were independent of the ligand used for the wash or the contact time, intercept values decreased about 2-fold between 1 and 30 min. This observation suggested that adsorption to the transport sites was reversible and that slow desorption kinetics were responsible for the positive intercept values. Under the assumption that the desorption was not mediated by the formation of a ternary complex with the ligand used in the extraction medium, these results correspond to a k'_d value for the Pb−L_{tr} complex of approximately 10^{-2}−10^{-3} s^{-1}. These values are noteworthy because they are only slightly faster than the value of k_{int} observed previously (4.3−6.6×10^{-4} s^{-1}). Nonetheless, they must be considered as a lower limit since they do not take into account the simultaneously occurring internalization process.

Influence of Ca on Pb Internalization. Competition experiments revealed that Pb uptake depended strongly on the concentration of Ca in the experimental medium. Pb uptake fluxes decreased by a factor 2 in the presence of a 100-fold excess of Ca and by a factor of 20 for a 1000-fold Ca excess. The Lineweaver−Burk linear transformation plots (Figure 8) demonstrated that Ca behaved as a competitive inhibitor by decreasing K_M without any influence on the maximum internalization flux (*25*). The binding affinity constant for Ca with L_{tr} was estimated to be $10^{4.65}$ M^{-1}, about 10 times lower than that observed for Pb. The observed competitive inhibition is in accordance with limited literature data (*26*), suggesting that lead can follow Ca transport pathways. Similar competition effects are often observed between nutrient and toxic metal ions (ref *2* and references therein), especially where the competing metals have similar ionic radii and coordination geometry.

Influence of Temperature on Pb Internalization. In an attempt to distinguish between Pb adsorption to the membrane receptors and internalization, experiments were also performed at 2 °C. Because binding to receptors is generally considered an exothermic process that is primarily driven by positive entropy changes (*27*, *28*), our hypothesis was that only small changes in equilibrium binding would be observed at the lower temperature, despite an important reduction in the internalization flux. Nonetheless, these considerations are complicated by the fact that both $\Delta H°$ and $\Delta S°$ may vary with temperature for protein−metal interactions (*29*). Indeed, in the presence of 9.7×10^{-8} M Pb, a decrease in temperature from 22 to 2 °C decreased both the internalization flux (5-fold) and the intercept values of the cellular Pb versus time plot ({Pb−L_{tr}}, 2.5-fold) in Figure 9. These results implied nearly equivalent decreases in K_{Pb-tr} and k_{int} and demonstrated that it was not possible to completely suppress Pb internalization at low temperature.

Numerical Simulation of Pb Uptake. Numerical simulation of the lead uptake process simultaneously considered diffusion in solution, adsorption to transport sites, and internalization (Figure 1). The flux equations employed and the values for each of the experimentally determined parameters were compiled in Table 2. Initial k_a values of 10^2−10^4 M^{-1} s^{-1} were estimated from the k'_d values obtained from the EDTA washing experiments and the stability constant (K_{tr}). Although k_a values were lower than would be determined under the assumption of the Eigen mechanism (10^{13} M^{-1} s^{-1}; *10*), the values are reasonable given the expected decrease in k_a due to steric constraints at the receptor binding site (*1*, *23*, *30*). Model parameters were optimized to experimentally obtained internalized and total cellular lead concentrations, i.e., both transport site bound Pb and internalized Pb.

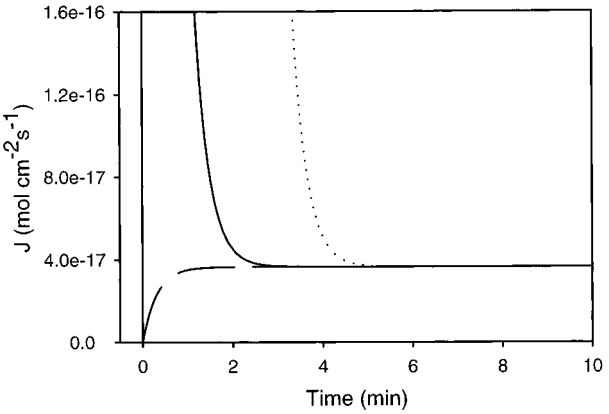

FIGURE 10. Modeled net adsorption flux (solid line); diffusion flux (dotted line); and internalization flux (dashed line) as a function of time, presented for first 10 min of the accumulation process for 9.7 $\times$ 10^{-8}M Pb at 22 °C (data from Figure 9). Optimized parameters were as follows: $k_{int} = 7 \times 10^{-4}$ s^{-1}, $k_a = 10^5$ M^{-1} s^{-1}, $\{L_{tr,tot}\} = 1.5 \times 10^{-11}$ mol cm^{-2}, and $K_{tr} = 3 \times 10^5$ M^{-1}.

Numerical simulations were performed for the cellular Pb temperature data (solid and dashed lines in Figure 9). The optimized model was found to give good agreement between experimentally obtained and model data for cellular lead concentrations and for concentration-dependent internalization fluxes between 5×10^{-9} and 5×10^{-5} M Pb^{2+}. As expected, adsorption was predicted to be extremely rapid with the maximal adsorption flux reached within a few seconds (Figure 10). Internalization fluxes were predicted to increase slightly in the initial stages of the experiment attaining constant values after about 1 min. Comparison of the different fluxes confirmed that mass transport and adsorption at the biological surface were relatively fast as compared to transport across the biological membrane. A similar method of numerical simulation that included efflux constants has been applied to describe the interaction between Zn and bacteria (*31*). In that case, Zn uptake was significantly faster than the Pb uptake observed here. Furthermore, inclusion of bacterial resistance mechanisms (efflux, production of extracellular complexing ligands) was necessary to explain the observed uptake data.

While the interpretation of flux measurements (*32*) is important in order to gain a better understanding of the basic mechanisms of cell functioning, a more important question is whether the basic assumptions of the simplified uptake models are likely to be satisfied in natural systems. The fundamental assumption in practically all of the simple approaches (e.g., FIAM, BLM) is that the steady state has been attained. Constant values of dissolved and adsorbed lead over the short-term experiments and the modeling results indicated that steady-state internalization fluxes were indeed attained within less than 1−1.5 min, thus supporting the validity of the approach in this case. Furthermore, the approach remains valid as long as cell numbers remain constant (verified here). Note that another, possibly more environmentally relevant approach, is to determine uptake fluxes by taking into account growth kinetics of the cell population using a modified Monod kinetics approach (*2*, *33*). In this case, cellular metal quotas are determined for steady-state populations of phytoplankton after long time periods. The disadvantage of this technique is that in laboratory experiments one must either precisely measure chemical speciation at steady-state or assume that no changes occur due to the presence of the plankton. This assumption is unlikely to be the case for many organisms (e.g., refs *31* and *34*).

Note finally that the biotic ligand model (*11*) assumes that organism-bound metal is related to biological effects through a proportionality between receptor-bound metal and uptake fluxes. The results presented here indicate that BLM results should be interpreted with caution since total body burdens (sum of the cellular and total adsorbed Pb in Figure 2) are not equivalent nor proportional to receptor-bound metal (Figure 5) even for this simple model organism. It is possible to speculate that the body burden approach would be more valid after system steady state is attained (Monod approach) than it is here for short equilibration times. Nonetheless, future experiments to verify the fundamental assumptions of the uptake process, especially in the presence of environmentally pertinent ligands and conditions, clearly warrant further study.

Acknowledgments

This work was supported, in part, by the Swiss National Funds 2000-050529.971 and the EU Project BIOSPEC (EVK1-CT-2001-000). We thank J. Buffle, J. Galceran, C. Hassler, P. Pinheiro, H. van Leeuwen, and three anonymous referees for helpful critical readings of initial versions of the paper and M. Martin for technical assistance.

Literature Cited

(1) Tessier, A.; Buffle, J.; Campbell, P. G. C. In *Chemical and Biological Regulation of Aquatic Systems*; Buffle, J., DeVitre, R., Eds.; Lewis Publishers: Boca Raton, FL, 1994; Chapter 6.
(2) Sunda, W. G.; Huntsman, S. A. *Sci. Total Environ.* **1998**, *219*, 165.
(3) Hudson, R. J. M. *Sci. Total Environ.* **1998**, *219*, 95.
(4) Hudson, R. J. M.; Morel, F. M. M. *Deep Sea Res.* **1993**, *40*, 129.
(5) Pasciak, W. J.; Gavis, J. *Limnol. Oceanogr.* **1974**, *19*, 881.
(6) Koch, A. L. *Adv. Microb. Ecol.* **1990**, *11*, 37.
(7) Bosma, T. N. P.; Middeldorp, P. J. M.; Schraa, G.; Zehnder, A. J. B. *Environ. Sci. Technol.* **1997**, *31*, 248.
(8) Ploug, H.; Stolte W.; Epping, E. H. G.; Jorgensen, B. B. *Limnol. Oceanogr.* **1999**, *44*, 1949.
(9) Campbell, P. G. C. In *Metal Speciation and Bioavailability in Aquatic Systems*; IUPAC Series on Analytical and Physical Chemistry of Environmental Systems, Vol. 3; Tessier, A., Turner, D., Eds.; John Wiley: Chichester, 1995; Chapter 2.
(10) Morel, F. M. M. *Principles of Aquatic Chemistry*; John Wiley: New York, 1984.
(11) Playle, R. C. *Sci. Total Environ.* **1998**, *219*, 147.
(12) Morel, F. M. M.; Hering, J. G. *Principles and Applications of Aquatic Chemistry*; John Wiley: Chichester, 1993; pp 405−414.
(13) Van Leeuwen, H. P. *Environ. Sci. Technol.* **1999**, *33*, 3743.
(14) Hudson, R. J. M. *Crit. Rev. Anal. Chem.* **1998**, *28*, 19.
(15) Pinheiro, J. P.; Van Leeuwen, H. P. *Environ. Sci. Technol.* **2001**, *35*, 894.
(16) Van Leeuwen, H. P.; Pinheiro, J. P. *J. Electroanal. Chem.* **1999**, *471*, 55.
(17) OECD Test Guideline 201.1984. Alga Growth Inhibition Test. In *OECD Guideline for Testing of Chemicals*; OECD Publications Office: Paris, France, 1984.
(18) Bates, S. S.; Tessier, A.; Campbell, P.; Buffle, J. *J. Phycol.* **1982**, *18*, 521.
(19) Martel, A. E.; Smith, R. M. *Critically Selected Stability Constants of Metal Complexes Data Base*, Version 5.0; Texas University: 1998.
(20) Martel, A. E.; Smith R. M. *Critical Stability Constants, Vol. 3*: *Other Organic Ligands*; Plenum Press: New York, 1977.
(21) Martel, A. E.; Smith R. M. *Critical Stability Constants, Vol. 6*: *Other Organic Ligands*; Plenum Press: New York, 1979.
(22) Errecalde, O.; Seidl, M.; Campbell, P. G. C. *Water Res.* **1998**, *32*, 419.
(23) Buffle, J. *Complexation Reactions in Aquatic Systems: An Analytical Approach;* Ellis Horwood: Chichester, 1988.
(24) Lauffenburger, D. A.; Linderman, J. I. *Receptors. Models for Binding, Trafficking and Signaling*; Oxford University Press: New York, 1993; Chapter 2.
(25) Stryer, L. *Biochemistry*; W. H. Freeman: New York, 1988.
(26) Simkiss, K.; Taylor, M. G. In *Metal Speciation and Bioavailability in Aquatic Systems*; IUPAC Series on Analytical and Physical Chemistry of Environmental Systems, Vol. 3; Tessier, A., Turner, D., Eds.; John Wiley: Chichester, 1995; Chapter 1.
(27) Klotz, I. M. *Q. Rev. Biophys.* **1985**, *18*, 227.
(28) Limbird, L. E. *Cell Surface Receptors: A Short Course on Theory and Methods*; Martinus Nijhoff Publishers: Boston, 1986.

(29) Hinz, H. *Annu. Rev. Biophys. Bioeng.* **1983**, *12*, 285.
(30) Stumm, W. *Aquatic Chemical Kinetics*; Wiley-Interscience: New York, 1990.
(31) Mirimanoff, N.; Wilkinson, K. J. *Environ. Sci. Technol.* **2000**, *34*, 616.
(32) Thellier, M.; Ripoll, C.; Vincent, J.-C.; Mikulecky, D. In *Some Physicochemical and Mathematical Tools for Understanding of Living Systems*; Greppin, H., Bonzon, M., Degli Agosti, K., Eds.; University of Geneva: Geneva, Switzerland, 1993; pp 221−277.
(33) Guttfreund, H. *Kinetics for Life Sciences: Receptors, Transmitters and Catalysts*; Cambridge University Press: Cambridge, 1995.
(34) Moffet, J. W.; Brand L. E. *Limnol. Oceanogr.* **1996**, *41*, 388.

Received for review June 5, 2001. Revised manuscript received November 7, 2001. Accepted November 22, 2001.

ES0101577